Design of all-pass operators for mixed phase deconvolution

Dorian Caraballo Ledesma CPGG/UFBA, and Milton J. Porsani, CPGG/IGEO/UFBA and INCT-GP/CNPQ/MCT

This paper was prepared for presentation at the Twelfth International Congress of the Brazilian Geophysical Society, held in Rio de Janeiro, Brazil, August 15-18, 2011.

Abstract

This paper present a new approach for mixed phase deconvolution. We investigate the use of arbitrary subsets of roots, distributed outside of the unit circle, to estimated mixed-phase inverse filter and wavelets. All pass filters are used to change the phase of the minimum phase filter. The influence of numbers of roots and its distributions was studied in order to obtain a optimum inverse mixed-phase filter. The optimization process to obtain the best inverse filter is performed by using a genetic algorithm. We have used the varimax norm as the object function to measure the simplicity of the deconvolved seismic trace. The method was tested using synthetic and real seismic data.

Introduction

An important task of the seismic deconvolution is to improve the temporal resolution and the spatial coherence of the reflections of the seismic traces. The conventional method is the well known minimum-phase or Wiener-Levinson (WL) deconvolution method. The classical assumptions of the WL method are: (i) the wavelet is stationary and minimum phase, (ii) the signal to noise ratio (S/N) is large, and (iii) the reflectivity is represented by a random process like white noise, implying that the autocorrelation function (ACF) of the seismic trace and the ACF of the seismic wavelet are equal unless a scale factor (Yilmaz, 1987).

The WL inverse filter is obtained in the least-squares sense by solving a system of normal equations (Robinson, 1980, Claerbout, 1985, Porsani e Ursin, 2007) giving a causal filter. Because mixed phase wavelet has also roots inside the unit circle so its inverse filter could not be causal. Consequently if the wavelet is not of minimum phase the WL filter produces a not good result (Leinbach, 1993).

In the last years several approach has being presented to the mixed-phase deconvolution problem. Porsani and Ursin, 1998 and Ursin and Porsani, 2000, purpose to use all pass filter to change the phase of the minimum-phase filter coupled with the genetic algorithm to select the best inverse filter. The all pass filter are formed by using roots estimated from the minimum-phase wavelet. Sacchi and Ulrych, 2000, Lu and Wang, 2007, Velis and Ulrych, 1996 uses higher-order statistics to retain phase information and non-minimum phase wavelets is estimated with cepstrum of the fourth-order cumulan. Levi and Oldenburg, 1982, and Baan, 2008, use a time-varying Wiener filtering approach to shows the phase changes of the seismic wavelet by constant phase rotation.

Deconvolution with mixed phase inverse filter generated from all-pass operator is very important because allows us to obtain phase information about the inverse filter and its corresponding wavelet. In the present paper we investigate the use of arbitrary subsets of roots, distributed outside of the unit circle, to estimated mixed-phase inverse filter and wavelet. Several configuration of roots outside of the unit circle was tested to generate all-pass filter. We study the influence of the number of the roots and its distribution respect to the unity circle in order to obtain inverse filters. To find the best inverse filter we use a genetic algorithm and to measure its performance we use the varimax norm of the deconvolved trace (Wiggins, 1978).

Convolution model and mixed phase inverse filter

The convolution model for the seismic trace x_t is the result of the convolution of the wavelet p_t with the reflectivity series r_t plus a random noise w_t.

$$x_t = p_t * r_t + w_t \tag{1}$$

The seismic wavelet in terms of the Z-transform may be represented as:

$$P(Z) = \sum_{j=0}^{N} p_j Z^j \tag{2}$$

A mixed phase wavelet $P(Z)$ has no zeros on the unit circle, β zeros inside the unit circle and $N-\beta$ zeros outside the unit circle, also has two component, minimum phase component $A(Z)$ and maximal phase component $Z^{\beta}B(Z^{-1})$,

$$P(Z) = A(Z)Z^{\beta}B(Z^{-1}) \tag{3}$$

Where the component are:

$$A(Z) = 1 + a_1 Z + \ \dots \ + a_{N-\beta} Z^{N-\beta} \tag{4}$$

$$B(Z^{-1}) = 1 + b_1 Z^{-1} + \ \dots \ + b_{\beta} Z^{-\beta} \tag{5}$$

Now, the minimum-phase seismic wavelet is:

$$\tilde{P}(Z) = A(Z)B(Z) \tag{6}$$

The wavelet components, $A(Z)$ and $B(Z)$ are both minimum phase, so the combination of the equation (3) and (6) is:

$$P(Z) = \tilde{P}(Z)\frac{Z^{\beta}B(Z^{-1})}{B(Z)} \tag{7}$$

We show that the mixed-phase wavelet in the equations (7) is the minimum phase wavelet convolved with an all-pass filter. The inverse filter of the mixed phase pulse with respect to the mixed-phase wavelet is:

$$H(Z) = \tilde{H}(Z)\frac{B(Z)}{Z^{\beta}B(Z^{-1})} \tag{8}$$

Design of all-pass operators and genetic algorithm

Now $B(Z)$ may be considered as an artificial minimum-phase wavelet of finite length. Let us to consider the roots of $B(Z)$ distributed outside of the unit circle forming a ring of roots (figure 1).

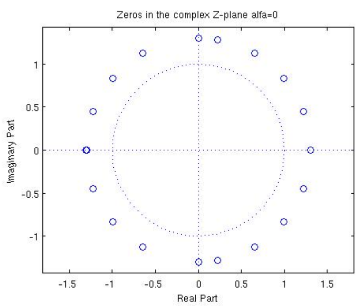

Figure 1: Diagram in the complex Z-plane showing the ring of roots outside of the unit circle ($|Z| = 1$), used to design all pass filters.

The polynomial $B(Z)$ have real roots $(r_{r,j})$ and pair of complex conjugate roots $(r_{c,j},\, r^{*}_{c,j})$,

$$\begin{aligned} {}^{\omega}B_j(Z) &= 1 + \tfrac{1}{r_{r,j}}Z \quad , \qquad j = 1, \ldots, \omega, \\ {}^{\gamma}B_j(Z) &= (1 + \tfrac{1}{r_{c,j}}Z)(1 + \tfrac{1}{r^{*}_{c,j}}Z) \quad , \qquad j = 1, \ldots, \gamma. \end{aligned} \tag{9}$$

$${}^{\beta}B_j(Z) = \prod_{j=1}^{\omega} {}^{\omega}B_j(Z) \prod_{j=1}^{\gamma} {}^{\gamma}B_j(Z), \qquad j = 1, \ldots, \beta \tag{10}$$

A genetic algorithm (GA) was used to evaluate an optimal mixed phase inverse filter. A binary chain of random bits $S_i, i = 1, \ldots \beta$, (see table 1.) is used to generate polynomials $B_i(Z)$ to form all-pass operators and mixed-phase inverse filters (eq. 8). The selected polynomials ${}^{\gamma}B_j(Z)$ and ${}^{\omega}B_i(Z)$ are indicated by the value one in table 1.

	${}^{\omega}B_1(Z)$	$\ldots$	${}^{\omega}B_{\omega}(Z)$	${}^{\gamma}B_1(Z)$	$\ldots$	${}^{\gamma}B_{\gamma}(Z)$
S_1	0	$\ldots$	1	1	$\ldots$	0
S_2	1	$\ldots$	0	1	$\ldots$	0
$\vdots$	$\vdots$	$\ldots$	$\vdots$	$\vdots$	$\ldots$	$\vdots$
S_{β}	1	$\ldots$	1	0	$\ldots$	1

Table 1. Schematic representation of the binary chain of random bits used to select roots outside unit circle (Fig. 1).

The $B_i(Z)$ is applied in the design of the inverse mixed phase filter (equation 8) and in the mixed phase wavelet (equation 7). The filter is convolved with the seismic trace and the objective function (varimax norm) is evaluated. During the generations of the GA, genetic operators are applied. The process is repeated up to the convergence. At the end the optimal mixed-phase inverse filter is selected as the one associated to the maximum value of the varimax norm.

Figure 2 shows the flowchart of the proposed method, where the all-pass operator and the filter Wiener-Levinson are combined to the designing of the mixed phase filter and the mixed phase wavelet.

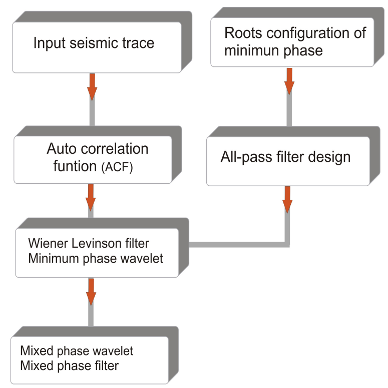

Figure 2: Flowchart for the design of the mixed phase filter and the wavelet.

Optimum mixed phase inverse filter and numerical results

The Figure 3 shows results of the minimum and mixed-phase inverse filters. Fig. 3a is a synthetic mixed phase wavelet, b) is the optimum mixed phase inverse filter, c) shows the deconvolution using the mixed phase filter. Figure 3d shows the WL minimum phase filter and Fig. 3e) shows the deconvolution of the mixed phase wavelet using the WL filter, producing the poor result.

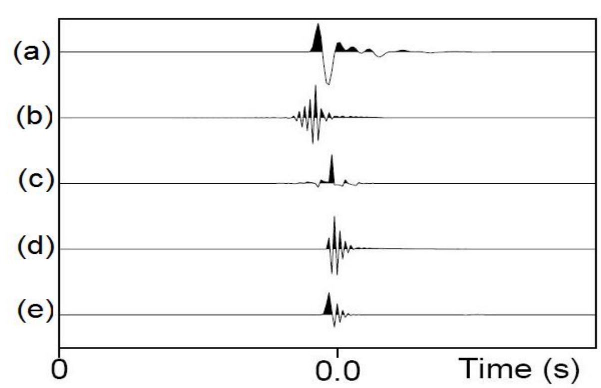

Figure 3: Deconvolution of a single mixed phase wavelet with the mixed phase inverse filter.

For each mixed phase filter we computed the performance criterium with the varimax norm, A genetic algorithm (GA) was implemented to select the best inverse filter used in Fig. 3. Figure 4 shows the evolution of the varimax norm during the GA, the curves for the maximum, minimum and mean values of the varimax norm indicate the convergence of the GA.

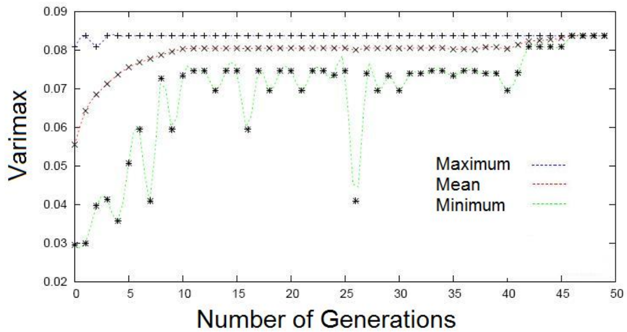

Figure 4: The performance of the genetic algorithm.

Figure 5 shows the results using to deconvolve a synthetic seismic trace. A random reflectivity series is shown in Fig. 5a, the synthetic mixed phase wavelet 5a. The synthetic seismic trace was obtained by convolving the reflectivity series with the mixed phase wavelet and the result is shown in 5c. The GA algorithm was used to obtain the optimal mixed phase inverse filter, see in 5e. The result of the deconvolution of the synthetic trace with the optimal filter is shwon in 5f. The result of the conventional minimum phase WL deconvolution is shown in 5e. Clearly the mixed phase deconvolution gives a better approximation of the reflectivity series.

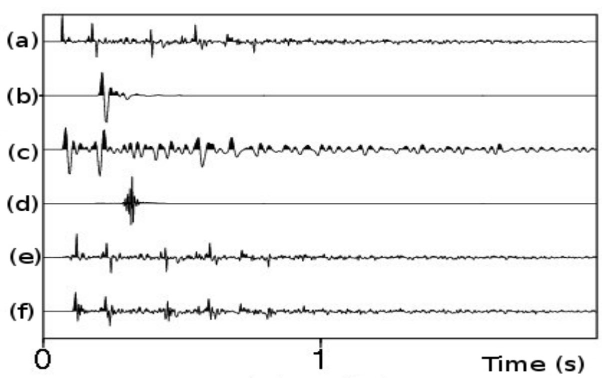

Figure 5: Deconvolution of a synthetic trace by using a optimal mixed phase inverse.

Wavelet estimation and deconvolution in the reservoir zone

Figure 6 shows a section of a 3D seismic data used to test the algorithm. In this example we estimate the wavelet and its corresponding inverse filter in a reservoir zone (Fig. 6). The seismic section is the crossline 834 passing through a well. A time-space window confining the reservoir was used to compute the ACF used to obtain the WL filter and to evaluate the objective function in the GA algorithm. The reservoir is confined between the time interval 1.0s to 1.8s.

Figure 7 shows the estimated minimum phase wavelet and the optimal mixed-phase wavelet in in (a) and (b), respectively. The mixed-phase inverse filter is shown in (c).

Figure 8a shows a seismic trace located at the well depicted in the figure 6. Results of the minimum and mixed-phase deconvolution are shown in (b) and (c), respectively.

Figure 9 shows results of the deconvolution of the selected time-space window. The original data is shown in (a) and results of the minimum and mixed-phase deconvolution are shown in (b) and (c), respectively. It may be observed (Fig. 9c) the better definition of the top of the reservoir (around 1.6 s) and some improvement in the lateral continuity of the reflections in the reservoir zone.

Figure 10 shows the amplitude spectrum of the data shown in Figs. 9a, 9b and 9c. We remark that the amplitude spectrum of the WL minimum-phase inverse filter and the optimal mixed phase inverse filter are equal, once the all pass filter only change the phase, equation (8).

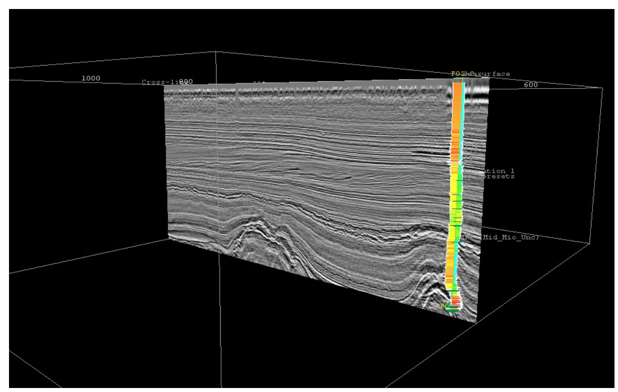

Figure 6: 3D seismic data, Netherlands Offshore F3 Block, Opendetect.

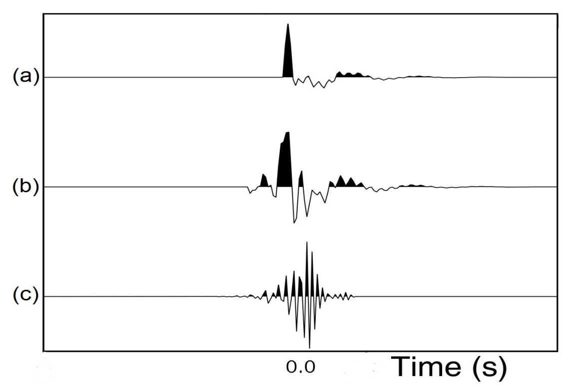

Figure 7: The estimated minimum phase wavelet in (a), the optimal mixed phase wavelet in (b) and the optimal mixed phase inverse filter in (c).

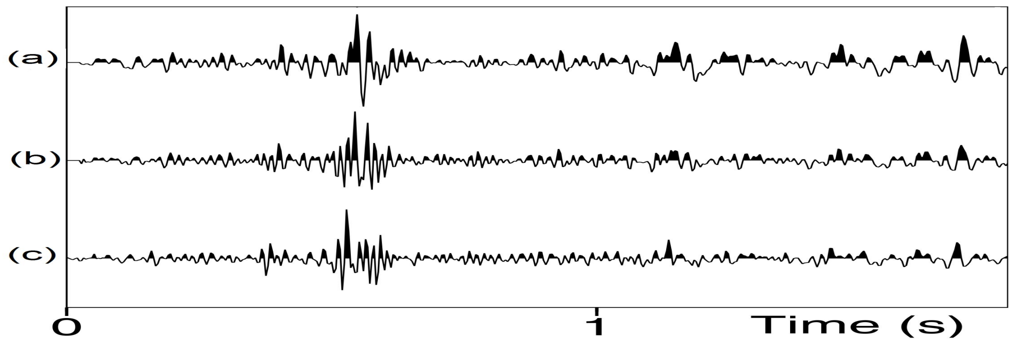

Figure 8: A real seismic trace in (a), result of minimum-phase deconvolution in (b) and the mixed-phase deconvolution in (c).

Conclusions

An new approach to obtain mixed phase inverse filter was presented. The mixed-phase inverse filters were generated using all-pass filter coupled with the classical Wiener-Levinson minimum-phase filter. A genetic algorithm was implemented to find the optimal filter.

Numerical results using synthetic and real 3D data demonstrated the enhancement of the lateral coherence of the reflections and the improvement in the time resolution on the seismic data.

References

Baan, M., 2008, Time varying wavelet estimation and deconvolution by kutorsis maximization: Geophysics, 73, V11-V18.

Claerbout, J. F., 1976, Fundamentals of geophysical data processing: McGraw-Hill, Inc.

Leinbach, J., 1993, Wiener spiking deconvolution and minimum phase wavelet: a tutorial: The Leading Edge, 14, 189-192.

Levi, S., and D. W. Oldenburg, 1982, The deconvolution of phase shifted wavelet: Geophysics, 47, 1285-1294.

Lu, X., and Y. Wang, 2007, Mixed-phase wavelet estimation by iterative linear inversion of high-order statistics: Geophysics, 6, 21-28.

Porsani, M.J., and B. Ursin, 1998, Mixed-phase deconvolution: Geophysics, 63, 637-647.

Porsani, M.J., and B. Ursin, 2007, Direct multichannel predictive deconvolution: Geophysics, 72, H11-H27.

Robinson, E.A., and S. Treitel, 1980, Geophysical Signal Analysis: Prentice-Hall, Inc.

Sacchi, M. D., and T. Ulrych, 2000, Non minimum phase wavelet estimation using higher order statistics: Leading Edge, 19, 80-83.

Ursin, B., and M.J. Porsani, 2000, Estimation of an optimal mixed-phase inverse filter: Geophysical Prospecting, 48, 663-676.

Velis, D. R., and T. Ulrych., 1996, Simulated annealing wavelet estimation via fourth-order cumulant matching: Geophysics, 61, 1939-1948.

Wiggins, R. A., 1978, Minimun entropy deconvolution: Geoexpl, 16 , 21-31.

Yilmaz, O., 1987. Seismic Data Processing: SEG, Tulsa.

Acknowledgments

The authors wish to express their gratitude to INCT-GP, PETROBRAS, FINEP, FAPESB and PRH8-ANP, for financial support. We also thanks PARADIGM, OPENDETECT and LANDMARK for the licenses granted to CPGG-UFBA.

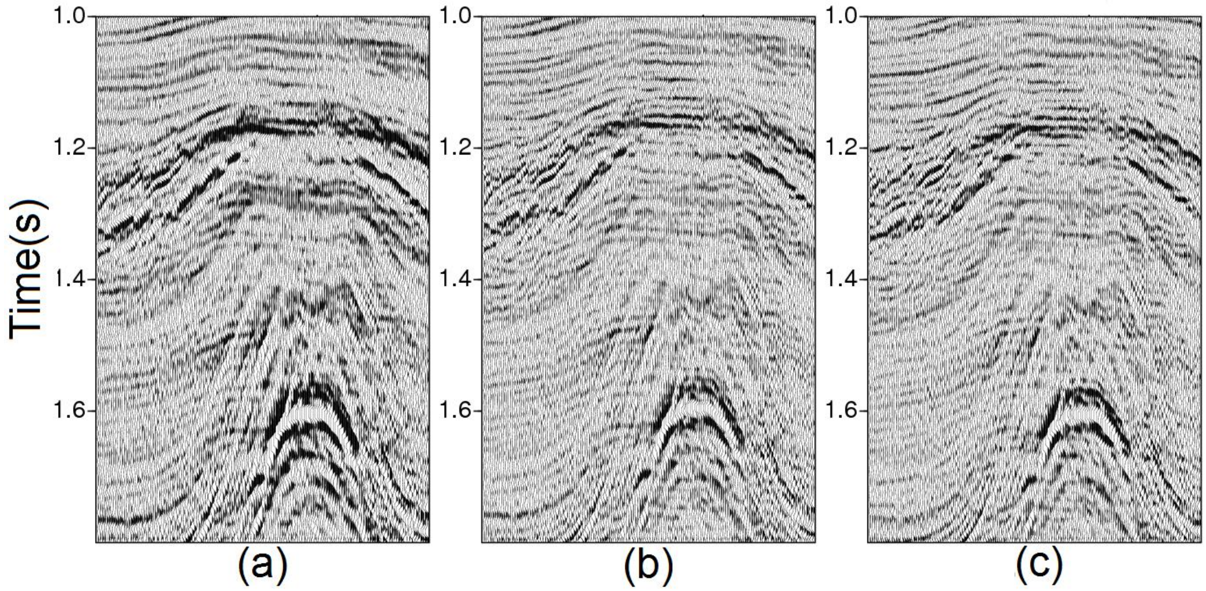

Figure 9: Results of the minimum and mixed-phase deconvolution of a seismic section with reservoir zone. Original data in (a) and results of the minimum and mixed-phase deconvolution in (b) and (c), respectively.

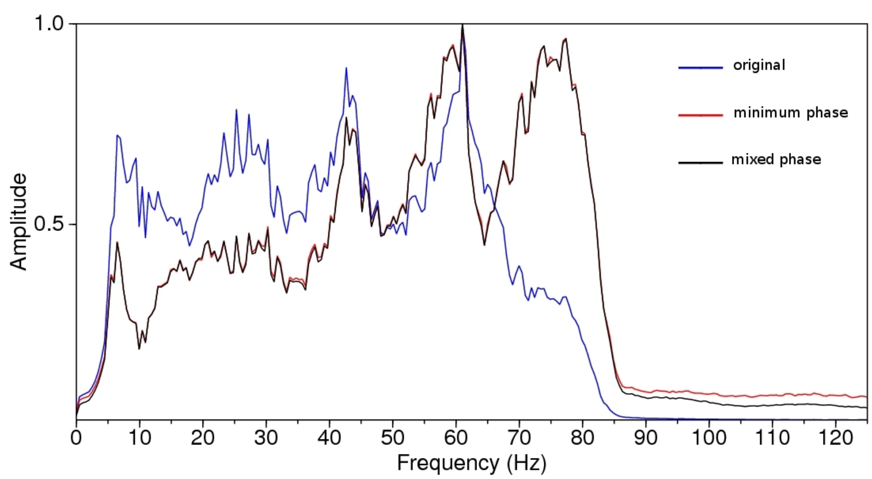

Figure 10: Average amplitude spectrum of data presented in Figs. 9a, 9c and 9c.